





## Article

# Cladding-Pumped Erbium/Ytterbium Co-Doped Fiber Amplifier for C-Band Operation in Optical Networks

Andis Supe <sup>1,\*</sup>, Sergejs Olonkins <sup>2</sup>, Aleksejs Udalcovs <sup>2</sup>, Ugis Senkans <sup>1</sup>, Rihards Mūrnieks <sup>1,3</sup>, Lilita Gegere <sup>1,2</sup>, Dmitrijs Prigunovs <sup>1,2</sup>, Jurgis Grube <sup>4</sup>, Edgars Elsts <sup>4</sup>, Sandis Spolitis <sup>1,3</sup>, Oskars Ozolins <sup>1,5</sup> and Vjaceslavs Bobrovs <sup>1</sup>

- <sup>1</sup> Institute of Telecommunications, Riga Technical University, 1048 Riga, Latvia; Ugis.Senkans@rtu.lv (U.S.); Rihards.Murnieks@rtu.lv (R.M.); Lilita.Gegere@rtu.lv (L.G.); Dmitrijs.Prigunovs@rtu.lv (D.P.); Sandis.Spolitis@rtu.lv (S.S.); Oskars.Ozolins@ri.se (O.O.); Vjaceslavs.Bobrovs@rtu.lv (V.B.)
- <sup>2</sup> AFFOC Solutions, 3016 Kalnciems, Latvia; Sergejs.Olonkins@rtu.lv (S.O.); aud@kth.se (A.U.)
- <sup>3</sup> Communication Technologies Research Center, Riga Technical University, 1048 Riga, Latvia
- <sup>4</sup> Institute of Solid State Physics, University of Latvia, 1063 Riga, Latvia; jurgis.grube@cfi.lu.lv (J.G.); Edgars.Elsts@cfi.lu.lv (E.E.)
- <sup>5</sup> Networks Unit, RISE Research Institutes of Sweden, 164 40 Kista, Sweden
- \* Correspondence: Andis.Supe@rtu.lv; Tel.: +371-25685880



**Citation:** Supe, A.; Olonkins, S.; Udalcovs, A.; Senkans, U.; Mūrnieks, R.; Gegere, L.; Prigunovs, D.; Grube, J.; Elsts, E.; Spolitis, S.; et al. Cladding-Pumped Erbium/Ytterbium Co-Doped Fiber Amplifier for C-Band Operation in Optical Networks. *Appl. Sci.* **2021**, *11*, 1702. <https://doi.org/10.3390/app11041702>

Academic Editor: Mirosław Klinkowski

Received: 15 January 2021  
Accepted: 10 February 2021  
Published: 14 February 2021

**Publisher's Note:** MDPI stays neutral with regard to jurisdictional claims in published maps and institutional affiliations.



**Copyright:** © 2021 by the authors. Licensee MDPI, Basel, Switzerland. This article is an open access article distributed under the terms and conditions of the Creative Commons Attribution (CC BY) license (<https://creativecommons.org/licenses/by/4.0/>).

**Abstract:** Space-division multiplexing (SDM) attracts attention to cladding-pumped optical amplifiers, but they suffer from a low pump power conversion efficiency. To address this issue, ytterbium (Yb<sup>3+</sup>) and erbium (Er<sup>3+</sup>) co-doping is considered as an effective approach. However, it changes the gain profile of Er<sup>3+</sup>-doped fiber amplifiers and induces the gain difference between optical wavelengths in the C-band, significantly limiting the effective band of the dense wavelength-division multiplexed (DWDM) system. This paper is devoted to a detailed study of a cladding-pumped Er<sup>3+</sup>/Yb<sup>3+</sup> co-doped fiber amplifier (EYDFA) through numerical simulations aiming to identify a configuration, before assembling a similar EYDFA in our laboratory premises that ensures the desired performance. The simulation model is based on a commercial double cladding EYDF whose parameters are experimentally extracted and fed to the EYDFA setup for the system-level studies. We investigate the wavelength dependence of the amplifier's characteristics (absolute gain, gain uniformity, noise figure) and bit error rate (BER) performance for several DWDM channels and their optical power. The obtained results show that a 7 m long EYDF and co-propagating pump direction is preferable for the EYDFA with a 3 W pump source at 975 nm and with the given gain medium characteristics for WDM applications. For instance, it ensures a gain of 19.7–28.3 dB and a noise figure of 3.7–4.2 dB when amplifying 40 DWDM channels with the input power of −20 dBm per channel. Besides, we study EYDFA gain bandwidth and the maximum output power when operating close to the saturation regime and perform a sensitivity analysis showing how the doped fiber's absorption and emission cross-sections impact the amplification process through energy transfer from Yb<sup>3+</sup> to Er<sup>3+</sup>. Finally, we quantify the power penalty introduced by the EYDFA; the results show that it is not higher than 0.1 dB when amplifying 40 × 10 Gbps non-return-to-zero on-off keying signals from −20 dBm/channel.

**Keywords:** bit error rate; cladding-pumped optical amplifier; doped fiber amplifiers; erbium/ytterbium co-doping; optical fiber network; simulation; wavelength division multiplexing

## 1. Introduction

An immense variety and accessibility of multimedia services, such as Netflix, YouTube, etc., together with optical fiber penetration in rural areas and growing numbers of end users, have caused a tremendous increase in internet traffic that now must be supported by telecom infrastructure [1,2]. This puts pressure on infrastructure providers, including optical network carriers. Therefore, they are looking for cost-efficient solutions able to support

them in the future and even in cases of global emergency. As the COVID-19 pandemic has shown, both telecom infrastructure providers and service providers get entrusted with a role of technological pillars, bonding humanity and supporting our society and business in daily activities such as remote work and distance education. Considering these aspects of growth rates of internet traffic, the versatility of broadband and multimedia services, as well as cost and energy efficiencies, space-division multiplexing (SDM) is considered as one of the biggest breakthroughs in fiber-optic communications able to support the sustainable evolution of telecom networks and services [3–5]. To ensure cost-efficient optical signal amplification in SDM-based fiber-optic transmission systems, cladding-pumped doped fiber amplifiers (DFAs) have attracted increased attention. They are considered as one of the most suitable amplification approaches from the perspective of both capital expenditure (CAPEX) and operational expenditure (OPEX) [6]. Such amplification schemes allow for using high-power uncooled multimode laser diodes as pumping sources, which significantly reduces the overall power consumption. Furthermore, the use of only one pumping source improves the cost-efficiency, helps to reduce the size of a multicore amplifier, and thus saves physical space in a rack when migrating to such an amplifier implementation [2].

Although multicore erbium-doped cladding-pumped fiber amplifiers (MC-EDFAs) are commonly used in SDM networks [2,7,8], they have an extremely low pump conversion efficiency. This is the main drawback of such amplifiers, which arises due to insufficient absorption of the pumping radiation by the gain medium [9]. Therefore, the increase in the output optical power is problematic. The typical output power values for MC-EDFAs are 14–17 dBm [10,11]. To overcome these limits, most of the current high-power optical fiber amplifiers use the gain media with erbium ( $\text{Er}^{3+}$ ) and ytterbium ( $\text{Yb}^{3+}$ ) co-doping. In this case, the amplification happens through two stages. In the first stage, the major part of 975 nm pumping radiation is absorbed by the  $\text{Yb}^{3+}$  that excites them to a state with higher energy. In the second stage, the excited  $\text{Yb}^{3+}$  resonantly transfer a portion of energy to  $\text{Er}^{3+}$  and excites them to a state with higher energy. In such a way, the absorption of the pumping radiation is significantly enhanced [12–14]. Furthermore, adding  $\text{Yb}^{3+}$  allows an increase in the separation between erbium ions in the gain medium, therefore,  $\text{Er}^{3+}/\text{Yb}^{3+}$  co-doping minimizes the possibility of clustering among  $\text{Er}^{3+}$ , thus allowing an increase in  $\text{Er}^{3+}$  concentration in the gain medium compared to the common implementation of erbium-doped fibers [9]. As the result, shorter lengths of  $\text{Er}^{3+}/\text{Yb}^{3+}$  co-doped fiber are required to achieve similar levels of amplification.

In recent years, cladding-pumped DFA solutions have been studied intensively to reveal the pros and cons that they potentially bring once deployed in SDM networks. In the following section, we briefly cover solutions that tackle the transmission performance limits [5,15], the wideband operation limits [16,17], and quantify their impact on network cost and energy efficiency performance [5,18]. For instance, a 40% power consumption reduction can be achieved by replacing the conventional core-pumped EDFAs with cladding-pumped 32-core EYDFAs [18]. Furthermore, the larger number of cores of MC amplifiers support larger savings. Similar conclusions are found in [5]; the authors have estimated that, by substituting all inline EDFAs in a 2230 km long loop between Paris and Marseille with cladding-pumped 12-core EYDFAs, the costs associated with signal amplification could be reduced by 33%. Moreover, a 55% reduction in the link's total power consumption would be achieved by the year 2035. Such significant cost and energy savings encourage the research in this area. A hero-experiment, demonstrating a 1 Pbps transmission over a 205 km long 32-core multicore fiber (MCF), is reported in [15] where an inline core-pumped 32-core EDFA is used for optical loss compensation. Remarkably, the authors mention that the amplifier's saturation (and not fiber nonlinearities and inter-core crosstalk (IC-XT)) was the main factor preventing the achievement of an even longer transmission. A cladding-pumped co-doped DFA addresses this issue at the expense of amplification bandwidth.

A wideband operation of MC-EDFAs, covering the C and the L optical bands, is studied in [16,17]. In the first case, a 19-core EDFA was used to achieve a 207 Tbps

transmission over a 1500 km long 12-core MCF. A transoceanic distance of more than 8000 km is demonstrated in [17] where the authors used a 31.4 km long recirculation loop, consisting of a 19-core MCF and two cladding-pumped MC-EDFAs (for the C and the L bands separately) for the inline amplification of the dual-polarization quadrature phase-shift keying (DP-QPSK) signals. When it comes to long-haul transmission, amplifier characteristics, e.g., noise figure (NF), gain profile, etc., can significantly decrease the number of amplification spans a signal can traverse before impairments degrade its quality below a certain threshold. Using the transmission link configuration with an MC-EYDFA and with a standard EDFA, the authors in [5] investigate the impact that the IC-XT has on the maximum transmission distance (without regeneration) when operating with the 400G dual-polarization 16-ary quadrature amplitude modulation (DP-16QAM). The investigation relies on the Gaussian noise (GN) model [19] to estimate the signal-to-noise ratio (SNR) after each 80 km long fiber span using the amplifier's NF and the IC-XT component. The results show that, for the considered scenario, the maximum transmission distance decreases from 11 spans to only eight spans when replacing the conventional inline EDFAs (NF = 4.5 dB) with the MC-EYDFAs (NF = 4.5 dB). For NF = 6.5 dB, the corresponding numbers are 11 and six spans, respectively. Therefore, the design of MC-EYDFAs should be carefully considered to reduce the impact on the maximum transmission distance while enabling cost and power savings. Yet, the impact that the design specifications of a cladding-pumped EYDFA (e.g., the length of  $\text{Er}^{3+}/\text{Yb}^{3+}$  co-doped fiber, pump power and propagation directions, and  $\text{Er}^{3+}/\text{Yb}^{3+}$  emission cross-sections) have on the amplifier's characteristics remain unclear, especially, when it comes to the wavelength dependence. This latter aspect is of importance for the use of such amplifiers to compensate optical losses in networks/links exploiting wavelength division multiplexing (WDM).

Therefore, in this article, we investigate the characteristics of an EYDFA under different operating conditions to assess the suitability for operation in a metro-access segment of optical transport networks where the dense wavelength-division multiplexing (DWDM) solutions are normally used. To perform the analysis, we have developed a simulation framework, consisting of a DWDM transmission system with up to  $64 \times 10$  Gbps DWDM channels allocated using the fixed 100 GHz grid and a single-core cladding-pumped EYDFA of our design. The amplifier's model is adjusted using the experimentally extracted characteristics (e.g., overlap factor, absorption, and emission cross-sections) of the commercial  $\text{Er}^{3+}/\text{Yb}^{3+}$  co-doped fiber. The fiber's core is rare-earth-doped phosphosilicate glass, the inner cladding is pure silica, and the outer cladding is fluorine-doped silica glass. The EYDFA performance is evaluated in terms of gain (G), noise figure (NF), and the output signal bit error ratio (BER). We analyze the wavelength dependence of these characteristics by varying the number of DWDM channels and their optical power levels and scaling the fiber's emission and absorption cross-sections. Furthermore, we quantify the power penalty due to the amplification of  $40 \times 10$  Gbps non-return-to-zero on-off keying (NRZ-OOK)-modulated wavelength channels. Note that a single-core configuration of the cladding-pumped EYDFA is used throughout the research to exclude distortions related to inter-core crosstalk (IC-XT) and cross-gain modulation and build a reference cladding-pumped EYDFA model for further studies.

The rest of the article is organized as follows. The simulation setup, alongside the description of the measurements and estimations of the gain medium parameters, is described in Section II. Section III analyzes the amplifier's performance under different operating conditions (number of DWDM channels, input optical power, absorption and emission characteristics of the  $\text{Er}^{3+}/\text{Yb}^{3+}$  doping) and quantifies the induced power penalty. Finally, Section IV summarizes the research findings.

## 2. Experimental Setup and Principles

The simulation setup used to characterize the performance of the developed cladding-pumped EYDFA is shown in Figure 1. It is realized using VPIphotonics Design Suite [20], yet the absorption and emission cross-sections of the  $\text{Er}^{3+}/\text{Yb}^{3+}$  co-doped phosphosilicate

glass double-cladding fiber are experimentally measured in our laboratory and fed as the input data to the simulation setup (Figure 1b). Besides, the overlap factor is estimated using the proposed red, green, blue (RGB) color approach applied to the EYDF cross-section images taken by a fiber microscope (Figure 2). As we assume that EYDFA will be operated in metro-access segments of optical transport networks, the multi-wavelength operation is considered. Consequently, the setup includes three parts: (i)  $n \times 10$  Gbps OOK WDM transmitters; (ii) the realistic model of our EYDFA, consisting of the EYDF itself, optical pump source (central wavelength  $\lambda_p = 975$  nm at 25 °C and output power 3–5 W), high-power optical combiners/splitters, and the amplifier’s test unit for the evaluation of its characteristics (e.g., gain spectrum and noise figure (NF)); and (iii) WDM (de-)multiplexers and receivers for signal quality estimation (not shown in Figure 1).

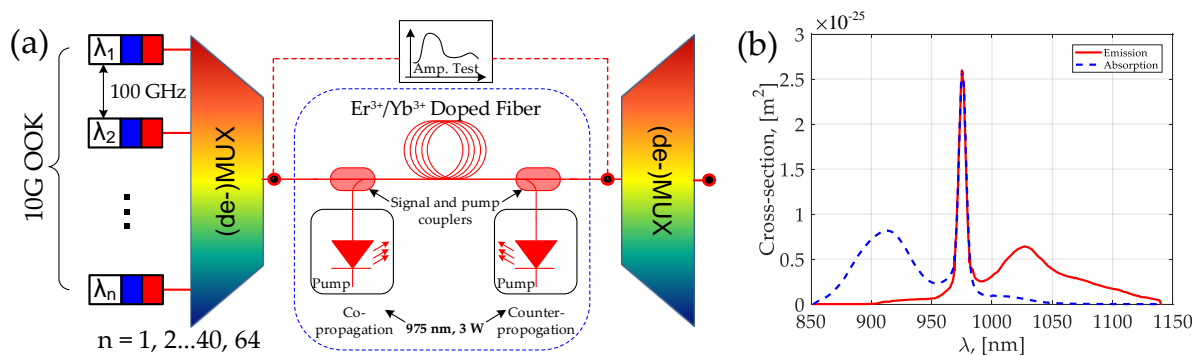


**Figure 1.** (a) Simplified simulation setup of the cladding-pumped  $\text{Er}^{3+}/\text{Yb}^{3+}$  co-doped fiber amplifier (EYDFA); (b) absorption and emission cross-sections experimentally determined for the  $\text{Yb}^{3+}/\text{Er}^{3+}$  co-doped fiber using the absorption spectra measurement method.

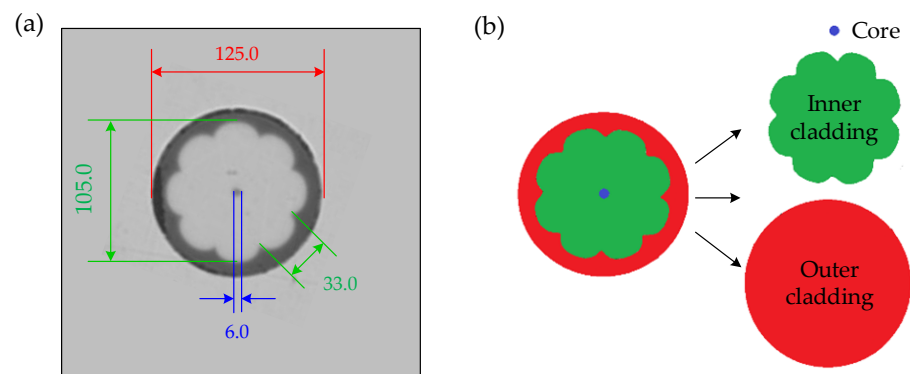


**Figure 2.** (a) Microscope image of the EYDF cross-section together with its geometrical measures, and (b) RGB representation of its outer cladding (red), inner cladding (green), and core (blue) used for the overlap factor estimation.

The key component of this optical back to back (OB2B) setup is a fiber model. For our purposes, we use a stationary fiber model from VPIphotonics Design Suite [20] that can be used for  $\text{Er}^{3+}/\text{Yb}^{3+}$  co-doped cladding-pumped fiber amplifiers. According to its description, this model is based on the bidirectional propagation equations for signals and multilevel rate equations for ion populations. To tune this model with the respect to our EYDF, we use the measured cross-sections to specify the emission and absorption spectra, and the overlap factors to specify the WDM signal ( $\sim 1550$  nm) and the pump signal ( $\sim 975$  nm) coupling and their propagation (which depends on fiber profile and dimensions). The model is resolved in both the longitudinal and transverse directions considering the number of effects, e.g.,  $\text{Er}^{3+}/\text{Yb}^{3+}$  energy transfer, cross-relaxation effects,

excited-state absorption, Rayleigh scattering, and Kerr nonlinearity. The summary of the setup parameters is given in Table 1.

**Table 1.** Summary of the amplifier’s schematic parameters.

System Parameters	
Bitrate and modulation	10 Gbps non-return-to-zero on-off keying
Number of channels ( $n$ )	1, 2, 4, 8, 16, 32, 40, 64 (41–64 outside of C-band)
The carrier frequency of the first/last channel	191.6/195.5 THz
Channel spacing	100 GHz
Single channel power	–25 dBm/channel to –10 dBm/channel
EYDFA Pump Parameters	
Pump wavelength	975 nm at temperature = 25 °C
Pump power	3 W, (operational range 0.3–5 W)
Direction	Co-/counter propagation
Doped fiber parameters	
Length	1–10 m
Er <sup>3+</sup> concentration	$1 \times 10^{25} \text{ m}^{-3}$
Yb <sup>3+</sup> concentration	$2 \times 10^{26} \text{ m}^{-3}$
Er <sup>3+</sup> /Yb <sup>3+</sup> cross-relaxation coefficient	$1 \times 10^{-22} \text{ m}^3/\text{s}$
Core area/inner cladding area ( $A_{\text{core}}/A_{\text{inner cladding}}$ )	0.0058
Inner cladding area/outer cladding area ( $A_{\text{inner cladding}}/A_{\text{outer cladding}}$ )	0.9203

The simulation model includes parameters that specify both the WDM system and the EYDFA under test. In this case, we operate with a 10 Gbps NRZ-OOK signal whose central frequencies are arranged across the C-band (1530–1565 nm) using a 100 GHz grid. Although we consider the WDM configuration with the total number of channels up to  $n = 64$ , channels 41–64 are outside of the C-band ( $f_c > 195.6$  THz). They are used to highlight the wavelength dependence of the amplifier’s gain and noise figure characteristics, especially for high ( $> -10$  dBm/channel) and low ( $< -25$  dBm/channel) input signal powers. The category “EYDFA pump parameters” provides details about the optical pump source and its direction with respect to the signal propagation. Finally, the category “doped fiber parameters” includes the measured, estimated, and given characteristics of our EYDF used to build the EYDFA in the laboratory.

To estimate the EYDF absorption cross-section, we use Er<sup>3+</sup> and Yb<sup>3+</sup> ion absorption spectra obtained using a measurement setup consisting of Agilent’s Cary 7000 Universal Measurement Spectrophotometer [21], FiberMate2™ Fiber Optic Coupler system from Harrick Scientific Products Inc. [22], and two EYDF samples of different lengths. A 1 m long EYDF sample is used to perform the absorption spectra measurements around a 975 nm wavelength, whereas a 19 m long sample was used for wavelengths around 1550 nm. In such a way, we avoid the saturation effect that might distort the absorption spectra measurements. The absorption around 975 nm is attributed to  $^2F_{7/2} \rightarrow ^2F_{5/2}$  and  $^4I_{15/2} \rightarrow ^4I_{11/2}$  optical transitions of Yb<sup>3+</sup> and Er<sup>3+</sup>, respectively. However, the impact of Er<sup>3+</sup> can be neglected since its absorption cross-section is significantly lower than that of Yb<sup>3+</sup> [23]. Furthermore, according to the specification, the EYDF has a 20 times higher Yb<sup>3+</sup> concentration compared to the Er<sup>3+</sup> concentration. The absorption cross-section is estimated using the measured absorption spectra, the ratio between the fiber’s core and

inner cladding areas, its length, and  $\text{Yb}^{3+}/\text{Er}^{3+}$  concentrations. The emission cross-section is estimated using the McCumber relation [24] connecting emission and absorption spectra.

Finally, the overlap factor is estimated using the RGB color approach that relies on the graphical post-processing of images of the doped fiber cross-section magnified by a microscope objective lens (see Figure 2). In general, the overlap factor ( $\Gamma$ ) of double-cladding optical fiber is defined as a ratio between its core area ( $A_c$ ) and inner cladding ( $A_{icl}$ ) area [25]:

$$\Gamma = \frac{A_c}{A_{icl}} \quad (1)$$

Since the inner cladding is usually formed into a specific shape (e.g., star shape [25], D shape [26], or even flower shape [27]), the estimation of its area becomes a task in itself since fiber manufacturers tend to provide only overall geometrical dimensions, whereas parameters such as core and cladding areas and ion concentrations, which are crucial when building and analyzing doped fiber amplifiers (DFAs), remain unrevealed. Similarly, in our case, the manufacturer of the EYDF provides information only about its geometrical dimensions (see Figure 2a) and the ratio between  $\text{Er}^{3+}/\text{Yb}^{3+}$  concentrations. Therefore, the overlap factor is estimated using the proposed RGB approach.

First, the gray-scale image from the microscope is used to identify the borders between the core, the inner cladding, and the outer cladding. Although this process may include a certain error due to the ambiguous edge detection of the fiber's core and inner cladding [28], it has an insignificant impact on the estimated overlap factor. When all edges are identified, an RGB color is assigned to each segment and they are recolored (see Figure 2b). The number of red (outer cladding), green (inner cladding), and blue (core) pixels are counted and used for the estimations.

For our EYDF,  $A_c = 658$  pixels,  $A_{icl} = 112,828$  pixels, and the outer cladding area  $A_{ocl} = 122,598$  pixels, which gives us  $\Gamma = 0.0058$  and  $A_{icl}/A_{ocl} = 0.9203$ . Both these parameters are further used as input to the simulation setup.

### 3. Results and Discussion

In this section, we reveal how the EYDFA's configuration parameters, such as the  $\text{Er}^{3+}/\text{Yb}^{3+}$  co-doped fiber's length, its absorption and emission cross-sections, and the pump signal direction, impact its wavelength-dependent characteristics, namely, gain uniformity, noise figure, and maximum output power. Before the evaluation of an EYDFA-induced power penalty, we characterize its performance for a multiwavelength scenario by varying the number of DWDM channels and their power levels. The goal of these simulations is to find the most appropriate amplifier configuration that introduces the least distortion while ensuring the most uniform gain spectrum possible. Throughout the analysis, we use an optical pump source operating at  $\lambda_p = 975$  nm and 3 W of output power. These values are selected based on the specifications of our high-power light source in the laboratory. We consider both the co-propagation and counter-propagation directions for the pump signal.

To select the length of the EYDF and the direction of the pump signal, we use the curves obtained for a 40-channel WDM system showing how the amplifier gain, noise figure, and the maximum output power change with the EYDF length (see Figure 3). The results show that the maximum gain is reached for an 8 m long EYDF regardless of the pump direction (Figure 3a). A longer EYDF does not result in a higher gain, which is explained by the depletion of the pump radiation. A further increase in doped fiber length not only cannot produce additional gain, but the amplified signal power also starts to decrease due to the attenuation of the EYDF itself. Furthermore, the amplifier becomes noisier, especially for the configuration where the signal and the pump are launched in the counter-propagating directions (Figure 3b). Otherwise, the noise figure is not larger than 4.5 dB (co-propagation) and 6 dB (counter-propagation). Finally, Figure 3c shows the maximum gain difference detected for Channels 1 to 40 (Ch1–Ch40) in the 40-channel DWDM system with the input optical power of  $-20$  dBm/channel.

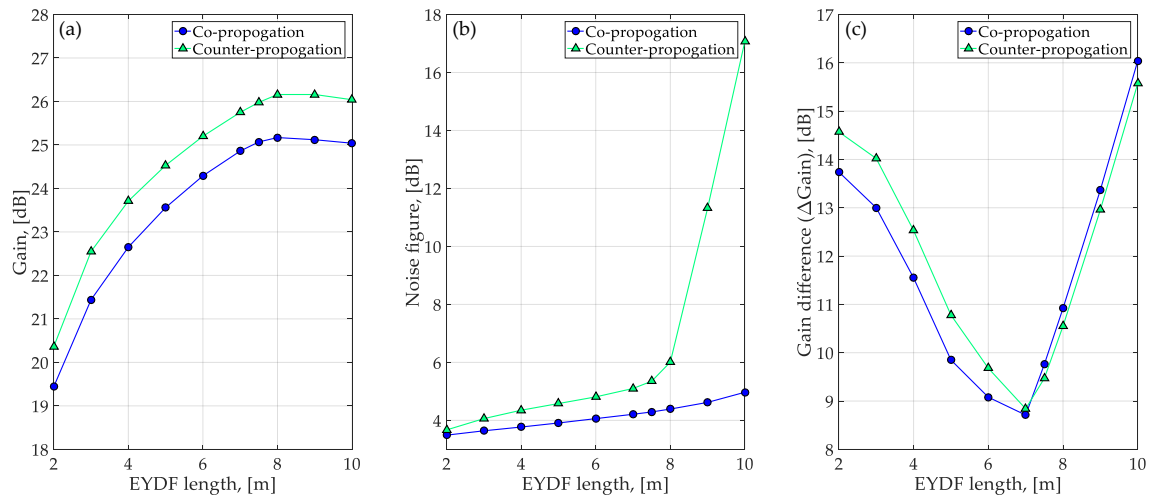


**Figure 3.** The amplifier’s (a) gain, (b) noise figure, and (c) maximum gain difference between the channels as a function of the EYDF length. Lines connecting data points are only included as a guide. The characteristics are obtained considering a 40-channel dense wavelength-division multiplexed (DWDM) system with an input optical power ( $p_{IN}$ ) of  $-20$  dBm/channel and a 3 W pump source at  $\lambda_p = 975$  nm coupled in the co-propagating (blue) and counter-propagating (green) directions.

The gain uniformity is an important characteristic, especially for systems with several amplification spans. Unless all DWDM channels are amplified equally, the power difference increases with every span, limiting the maximum transmission distance. The smallest gain difference ( $\Delta G < 9$  dB) is obtained for a 7 m long EYDF for both the co-propagation and counter-propagation of the 975 nm pump signal. It is significantly larger for shorter and longer EYDF segments, which indicates that an appropriate level of ion population inversion is achieved for this specific combination of the pump power (3 W) and the EYDF length (7 m). Therefore, we keep these parameters unchanged. Finally, we choose to use the pump signal in the co-propagation direction. Although the counter-propagation ensures a 0.9–1 dB higher gain, its cost is a higher noise figure, which is almost 1 dB higher compared to the co-propagation case. Therefore, we choose a lower noise figure over a higher gain. Figure 4a shows the output (parametrized) spectrum, whereas Figure 4b shows the individual gain and noise figure of each EYDFA-amplified DWDM channel. Due to the wavelength-dependent gain and noise figure of the amplifier, the output spectrum is not uniform. Specifically, the amplifier’s output power levels change from 0.1 to 8.3 dBm per channel (dBm/channel, see Figure 4a), resulting in a gain difference of 19.7–28.3 dB, and the noise figure changes from 3.7 dB to 4.2 dB (Figure 4b). The input optical power ( $p_{IN}$ ) was set to  $-20$  dBm/channel in all 40 WDM channels considered.

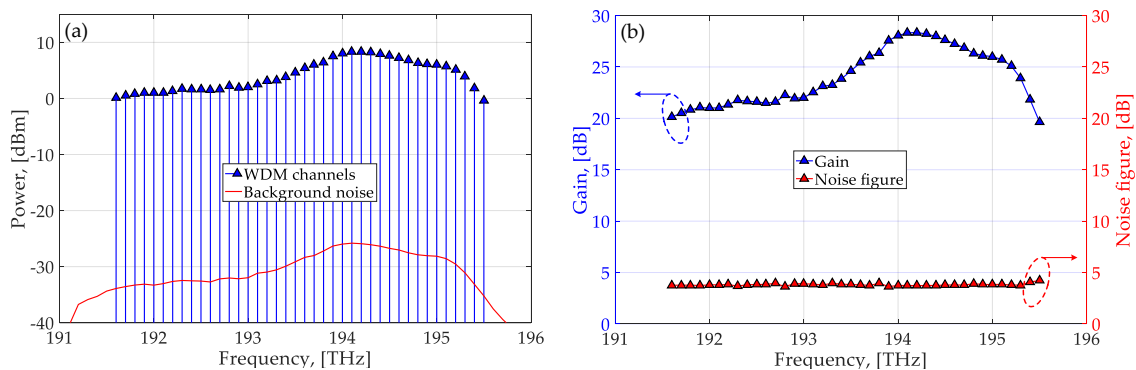


**Figure 4.** (a) Optical spectrum at the output of the EYDFA (7 m EYDF, 3 W, 975 nm, co-propagation), (b) individual gain and noise figure of each amplified DWDM channel with  $p_{IN} = -20$  dBm/channel.

Next, we explore the EYDFA characteristics (namely gain, maximum gain difference, and noise figure) under different operating conditions by varying the number of DWDM channels and their optical power levels. During the analysis, we consider a DWDM configuration with 1, 2, 4, 8, 16, 32, 40, and 64 channels, whose power levels are set between  $-25$  and  $-10$  dBm/channel, see Figure 5. The output power curves (Figure 5a) show that the higher the number of DWDM channels, the smaller the output power difference. The amplifier saturates and eventually it fails to amplify more than 40 DWDM channels even if their power is as low as  $-25$  dBm/channel. When analyzing the output power curve for  $p_{IN} = -25$  dBm/channel, we have noticed that the output power levels increase by 3.5 dB when the number of DWDM channels is increased from two to four. However, the corresponding number is 4.3 dB when the number of DWDM channels is increased from 16 to 32 channels. Such behavior indicates that low-power optical signals (i.e., with low input power and/or a small number of channels) are not able to completely exploit the population inversion generated in the gain media. Consequently, the unused portion of the population inversion eventually generates an excessive amount of amplified spontaneous emission (ASE) noise, which results in a poor noise figure, see Figure 5c. On the contrary, high input power consumes the achieved population inversion, in such a way that the obtained gain is reduced and the output power reaches its limit. For instance, the output power increases by 0.3 dB when an additional eight channels ( $p_{IN} = -25$  dBm/channel) are added to a DWDM system with 32 channels, and it remains similar even when the number of channels is increased to 64. A higher pump signal power also does not result in a higher gain or a higher output power. Even if a 4 W pump signal is used, the output power increases by not more than 0.2–0.3 dB for a 40-channel configuration with  $p_{IN} = -20$  dBm/channel. Therefore, the maximum output power of the proposed EYDFA is limited to approximately 22 dBm.

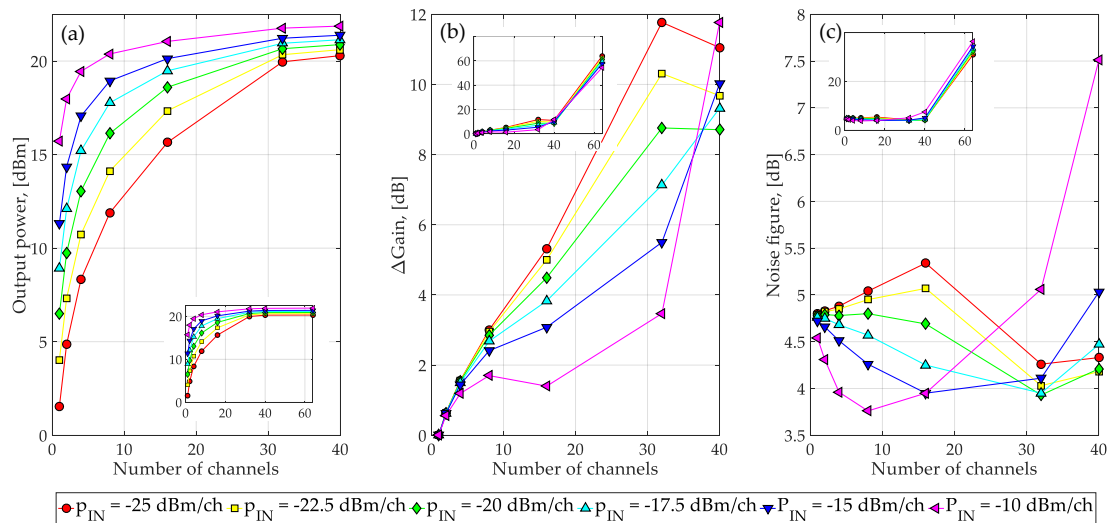


**Figure 5.** (a) Output power, (b) maximum gain difference, and (c) maximum noise figures vs. the number of DWDM channels and their input power for the EYDFA configuration with a 7 m long EYDF and  $p_{PUMP} = 3$  W at  $\lambda_p = 975$  nm coupled in the co-propagation direction. Lines connecting data points are only included as a guide.

The maximum gain difference curves (Figure 5b) show the following trend—the higher the input power, the smaller the gain difference in a DWDM system with 4–32 channels. The main reason is that a higher portion of population inversion is consumed to achieve similar levels of amplification for higher input power signals. Therefore, at a certain level of population inversion, optical signals with higher power get less amplified and the gain difference between the channels becomes smaller. However, the opposite situation is observed for 40 DWDM channels, where the gain difference becomes higher for higher input signal powers (e.g., compare  $-25$  dB/channel and  $-10$  dB/channel curves). Such behavior



occurs because higher power signals drain the ion population inversion more efficiently. The increase in the DWDM channel count to 40 in the case of a  $-25$  dBm input signal changes the average level of population inversion throughout the EYDF to a value that provides more equal gain in the transmission system frequency band. Therefore, we observe a more uniform gain (amplification) of all 40 DWDM channels with  $p_{IN} = -25$  dBm/channel, whereas for  $-10$  dBm/channel, the population inversion is drained much faster before the similar uniformity is achieved. A similar tendency is observed for the EYDFA's noise figure (Figure 5c). For channels with  $p_{IN} \geq -20$  dBm/channel, the noise figure first decreases with every additional DWDM channel until the number of channels (and their combined power level) reaches a certain optimum point, exceeding which the noise figure starts increasing. For fewer power channels, the noise figure first increases by 0.5–1 dB and then starts decreasing, reaching 4–4.5 dB for 32–40 DWDM channels. The insets in Figure 5b,c show that the gain difference and the noise figure increasing dramatically when the number of DWDM channels exceeds 40, which confirms the bandwidth limitations of the amplifier. Signals outside the operation band get absorbed by the EYDF.

In  $Er^{3+}/Yb^{3+}$  co-doped fibers,  $Yb^{3+}$  absorb the pump radiation and then resonantly transfer a portion of their energy to  $Er^{3+}$  for signal amplification. We perform a sensitivity analysis showing how the absorption and the emission cross-sections of our EYDF impact the amplification process. For this purpose, we assume the cross-sections to be 70% ( $k = 1$ ) and 130% ( $k = 1.3$ ) of the initially estimated values ( $k = 1$ ). Figure 6 shows the differences in the performance characterized using the excited ion percentage (Figure 6a), per channel gain, and noise figure (Figure 6b). We observe that, for  $k = 0.7$ , the peak of the excited  $Yb^{3+}$  percentage becomes smaller (approximately by 5%) and moves further into the EYDF by changing its axial position. Consequently, the depletion of the population inversion is smoothed out on all energy levels, allowing the amplified signal to accumulate a certain part of the pump energy and therefore improving its ability to consume larger portions of the population inversion. This extends the length of the EYDF where the signal amplification occurs effectively, leading to a higher gain (by  $\sim 0.7$  dB) and a lower noise figure (by  $\sim 0.1$  dB). On the contrary, for larger cross-sections ( $k = 1.3$ ), the  $Yb^{3+}$  peak moves towards the signal/pump source (axial position = 0.7 m) and gets smoothed out, which brings a lower gain and a higher noise figure.

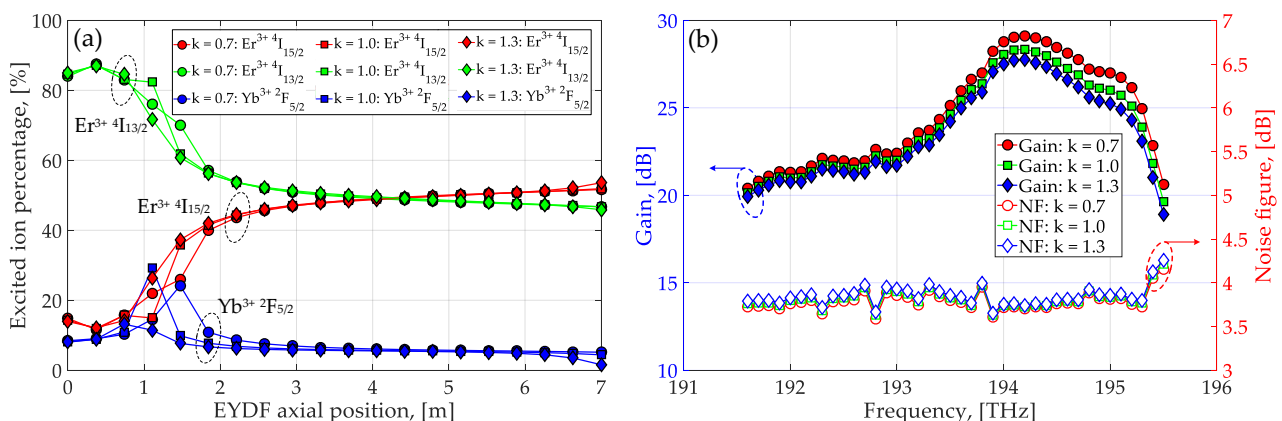


**Figure 6.** Sensitivity analysis showing the impact that the fiber's absorption and emission cross-sections have on ion excitation for coefficients  $k = 0.7, 1, 1.3$  of the initially estimated cross-section values: (a) excited ion percentage vs. axial position in the doped fiber; (b) the EYDFA average gain and the maximum noise figure of the 40-channel DWDM system.

Finally, the BER performance is evaluated for a 40-channel configuration of the DWDM system with and without the EYDFA (see Figure 7). The BER values are obtained for four channels: Ch1 with  $f_c = 191.6$  THz (the beginning of the C-band), Ch16 with  $f_c = 193.1$  THz (the anchor frequency of the DWDM grid), Ch26 with  $f_c = 194.1$  THz (gives the peak gain), and Ch40 with  $f_c = 195.5$  THz (the end of the C-band), but Figure 7 shows the largest

BER at a particular value of the received power. To obtain statistically reliable results, we use a  $2^{15}-1$  uniquely seeded pseudorandom binary sequence (PRBS) to obtain  $2^{13}$  bits used for the simulations and BER estimation that relies on the stochastic signal and noise representation. Specifically, the noise is added to the signal and the probability density function of the detected signal is approximated with the chi-square function. The EYDFA parameters remain unchanged (7 m EYDF, 3 W, 975 nm, co-propagation), and the input optical power is set to  $-20$  dBm per WDM channel.

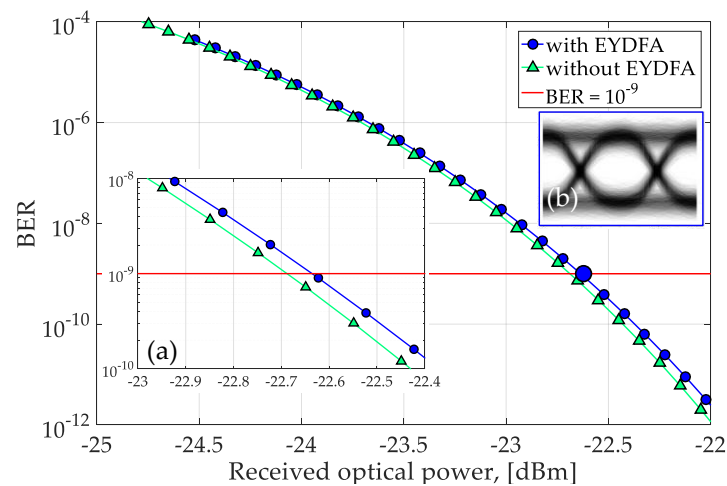


**Figure 7.** The worst bit error rate (BER) vs. received optical power detected for Ch1 = 191.6 THz, Ch16 = 193.1 THz, Ch26 = 194.1 THz, and Ch40 = 195.5 THz in a 40-channel WDM system ( $P_{IN} = -20$  dBm/channel) with and without the EYDFA where inset (a) zooms into the area at  $BER = 10^{-9}$  and inset (b) shows the eye diagram captured for the configuration with the amplifier at  $BER \cong 10^{-9}$ .

The results in Figure 7 shows the power penalty below 0.1 dB at the reference level of  $BER = 10^{-9}$  compared to the configuration without the amplification. Such distortion levels can be considered as negligible. However, its gain spectra should be flattened out, e.g., by using gain flattening filters or several amplification stages, before such amplifiers can be efficiently used for optical loss compensation in WDM transmission systems. However, this aspect deserves separate attention and thus will be addressed in future work.

#### 4. Conclusions

The performance of the cladding-pumped EYDFA is characterized using the developed measurement data-based simulation framework. Through the analysis of the amplifier's gain, noise figure, and power penalty, we assess its suitability for operation in metro-access optical transport networks where DWDM techniques are normally deployed. First, we experimentally characterize the double cladding  $Er^{3+}/Yb^{3+}$  co-doped fiber used as a gain medium for our amplifier to come up with the realistic model of the EYDF. Next, we test different EYDFA configurations under different operating conditions (including various doped fiber lengths, pump propagation directions, signal input power, etc.) to reveal parameter settings ensuring the best amplification characteristics, namely, high and uniform gain, and low noise figure. Finally, its power penalty is quantified using  $40 \times 10$  Gbps NRZ-OOK signals and the DWDM system configuration with and without the EYDFA. The results show that the amplifier configuration with a 3 W pump source at 975 nm requires a 7 m long EYDF (with the obtained physical parameters) and a co-propagation pumping direction for WDM applications. Considering a reasonably low input signal power ( $\sim -20$  dBm/channel), the EYDFA can be used to amplify up to 40 DWDM channels across the C-band, ensuring a maximum output power of +22 dBm, a gain of 19.7–28.3 dB, a noise figure of 3.7–4.2 dB, and a power penalty (with respect to a system without amplification) below 0.1 dB at a BER level of  $10^{-9}$ . Finally, the performed

sensitivity analysis for EYDF cross-sections shows how the energy transfer from Yb<sup>3+</sup> to Er<sup>3+</sup> ions impacts the amplifier's gain and noise figure values. Specifically, a ±30% change in the cross-sections results in minor gain and noise figure changes—0.7 dB and 0.1 dB, respectively. The revealed characteristics are of importance for assembling and testing an in-house-made cladding-pumped EYDFA.

**Author Contributions:** Conceptualization, A.S., S.O., A.U., R.M., S.S., V.B.; methodology, A.S., S.O., A.U., U.S., D.P., V.B.; software, S.O., A.U., L.G., R.M., J.G., E.E.; validation, U.S., D.P., L.G., J.G., E.E., O.O.; formal analysis, S.O., U.S., D.P., L.G., O.O., V.B.; investigation, A.S., S.O., A.U., R.M., J.G., E.E., S.S., O.O.; resources, S.S., O.O., V.B.; data curation A.S., S.O., A.U., U.S., D.P., L.G.; writing—original draft preparation, A.S., S.O. and A.U.; writing—review and editing, S.O., A.U., R.M., J.G., S.S., O.O., V.B.; visualization, A.S., S.O., A.U., S.S., J.G.; supervision, S.S., O.O., V.B.; project administration S.S., V.B.; funding acquisition S.S., J.G., V.B. All authors have read and agreed to the published version of the manuscript.

**Funding:** This work has been supported by the European Regional Development Fund project No. 1.1.1.1/18/A/068.

**Institutional Review Board Statement:** Not applicable.

**Informed Consent Statement:** Not applicable.

**Acknowledgments:** The Institute of Solid State Physics, University of Latvia as a Center of Excellence has received funding from the European Union's Horizon 2020 Framework Programme H2020-WIDESPREAD-01-2016-2017-TeamingPhase2 under grant agreement No. 739508, project CAMART<sup>2</sup>.

**Conflicts of Interest:** The authors declare no conflict of interest.

## References

1. Cisco Inc. *Cisco Annual Internet Report (2018–2023)*; Cisco: San Jose, CA, USA, 2020.
2. Yoshikane, N.; Tsuritani, T. Recent progress in space-division multiplexing optical network technology. In Proceedings of the 2020 International Conference on Optical Network Design and Modeling (ONDM), Barcelona, Spain, 18–21 May 2020; pp. 1–4.
3. Puttnam, B.J.; Sugizaki, R.; Rademacher, G.; Luis, R.S.; Eriksson, T.A.; Klaus, W.; Awaji, Y.; Wada, N.; Maeda, K.; Takasaka, S. High data-rate and long distance mcf transmission with 19-core C+L band cladding-pumped EDFA. *J. Light. Technol.* **2020**, *38*, 123–130. [[CrossRef](#)]
4. Jain, S.; Thipparapu, N.K.; Barua, P.; Sahu, J.K. Cladding-pumped Er/Yb-doped multi-element fiber amplifier for wideband applications. *IEEE Photon. Technol. Lett.* **2015**, *27*, 356–358. [[CrossRef](#)]
5. Thouras, J.; Pincemin, E.; Amar, D.; Gravey, P.; Morvan, M.; Moulinard, M.-L. introduction of 12 cores optical amplifiers in optical transport network: Performance study and economic impact. In Proceedings of the 2018 20th International Conference on Transparent Optical Networks (ICTON), Bucharest, Romania, 1–5 July 2018; pp. 1–4.
6. Ono, H.; Takenaga, K.; Ichii, K.; Yamada, M. Amplification technology for multi-core fiber transmission. In Proceedings of the 2014 IEEE Photonics Society Summer Topical Meeting Series, Montreal, QC, Canada, 14–16 July 2014; pp. 146–147.
7. Takeshima, K.; Tsuritani, T.; Igarashi, K.; Morita, I.; Tsuchida, Y.; Maeda, K.; Saito, T.; Watanabe, K.; Sasa, T.; Imamura, K.; et al. WDM/SDM transmission of 76 × 128-Gbit/s Nyquist-pulse-shaped DP-QPSK Signals over 4,200 km using cladding pumped 7-Core EDFA. In Proceedings of the 2015 Opto-Electronics and Communications Conference (OECC), Shanghai, China, 28 June–2 July 2015; pp. 1–3.
8. Matsumoto, K.; Seno, K.; Mizuno, T.; Yanagimachi, S.; Gaborv, E.L.T.D.; Mivamoto, Y. Experimental demonstration of a SDM node with low power consumption MC-EDFA and SPOC-based WSS arrays. In Proceedings of the 2019 24th OptoElectronics and Communications Conference (OECC) and 2019 International Conference on Photonics in Switching and Computing (PSC), Fukuoka, Japan, 7–11 July 2019; pp. 1–3.
9. Baker, C.C.; Burdett, A.; Friebele, E.J.; Rhonehouse, D.L.; Kim, W.; Sanghera, J. Rare earth co-doping for increased the efficiency of resonantly pumped Er-fiber lasers. *Opt. Mater. Express* **2019**, *9*, 1041–1048. [[CrossRef](#)]
10. Ono, H. Gain Control in Multi-core EDFA with hybrid-pumping. In Proceedings of the 2019 24th OptoElectronics and Communications Conference (OECC) and 2019 International Conference on Photonics in Switching and Computing (PSC), Fukuoka, Japan, 7–11 July 2019; pp. 1–3.
11. Sugizaki, R. Recent technologies on multicore EDFA. In Proceedings of the 2018 IEEE Photonics Society Summer Topical Meeting Series (SUM)—IEEE Photonics Conference, Reston, VA, USA, 30 September–4 October 2018; pp. 261–262. [[CrossRef](#)]
12. Wei, S.; Yao, B.; Chen, Y.; Mao, Q. Cladding-Pumped Erbium-Ytterbium Co-Doped Fiber Amplifier with Dual-Wavelength Auxiliary Signal Injection of 1030 and 1040 nm. *IEEE Photonics J.* **2020**, *12*, 1–9. [[CrossRef](#)]
13. Anashkina, E.A. Laser sources based on rare-earth ion doped tellurite glass fibers and microspheres. *Fibers* **2020**, *8*, 30. [[CrossRef](#)]

14. Koptev, M.Y.; Anashkina, E.A.; Bobkov, K.K.; Likhachev, M.E.; Levchenko, A.E.; Aleshkina, S.S.; Semjonov, S.L.; Denisov, A.N.; Bubnov, M.M.; Lipatov, D.S.; et al. Fibre amplifier based on an ytterbium-doped active tapered fibre for the generation of megawatt peak power ultrashort optical pulses. *Quantum Electron.* **2015**, *45*, 443–450. [[CrossRef](#)]
15. Kobayashi, T.; Nakamura, M.; Hamaoka, F.; Shibahara, K.; Mizuno, T.; Sano, A.; Kawakami, H.; Isoda, A.; Nagatani, M.; Yamazaki, H.; et al. 1-Pb/s (32 SDM/46 WDM/768 Gb/s) C-band dense SDM transmission over 205.6-km of single-mode heterogeneous multi-core fiber using 96-Gbaud PDM-16QAM channels. In Proceedings of the Optical Fiber Communication Conference Postdeadline Papers, Los Angeles, CA, USA, 19–23 March 2017; p. Th5B.1.
16. Soma, D.; Beppu, S.; Maeda, K.; Takasaka, S.; Suqizaki, R.; Takahashi, H.; Tsuritani, T. Long-haul MCF transmission using full C+L-band 19-core cladding-pumped EDFA. In Proceedings of the 2018 European Conference on Optical Communication (ECOC), Rome, Italy, 23–27 September 2018; pp. 1–3.
17. Puttnam, B.; Rademacher, G.; Luís, R.; Eriksson, T.; Klaus, W.; Awaji, Y.; Wada, N.; Maeda, K.; Takasaka, S.; Sugizaki, R. 8007 km C + L band transmission over MCF with 19-core cladding-pumped EDFA. In Proceedings of the 45th European Conference on Optical Communication (ECOC 2019), Dublin, Ireland, 23–25 September 2019; pp. 1–4.
18. Jain, S.; Castro, C.; Jung, Y.; Hayes, J.; Sandoghchi, R.; Mizuno, T.; Sasaki, Y.; Amma, Y.; Miyamoto, Y.; Bohn, M.; et al. 32-core erbium/ytterbium-doped multicore fiber amplifier for next generation space-division multiplexed transmission system. *Opt. Express* **2017**, *25*, 32887–32896. [[CrossRef](#)]
19. Poggiolini, P.; Bosco, G.; Carena, A.; Curri, V.; Jiang, Y.; Forghieri, F. The GN-model of fiber non-linear propagation and its applications. *J. Light. Technol.* **2013**, *32*, 694–721. [[CrossRef](#)]
20. VPiPhotonics GmbH. VPiTransmissionMaker 11.0. Available online: <https://www.vpiphotonics.com/> (accessed on 10 December 2020).
21. Agilent Cary 7000 Universal Measurement Spectrophotometer. Available online: <https://www.agilent.com/en/product/molecular-spectroscopy/uv-vis-uv-vis-nir-spectroscopy/uv-vis-uv-vis-nir-accessories/cary-universal-measurement-accessory-uma> (accessed on 12 December 2020).
22. Harrick Scientific Products Inc., FiberMate2™ Fiber Optic Coupler System. Available online: <https://www.harricksci.com/ftir/accessories/group/FiberMate2%E2%84%A2-Fiber-Optic-Coupler> (accessed on 12 December 2020).
23. Huang, F.; Liu, X.; Ma, Y.; Kang, S.; Hu, L.; Chen, D. Origin of near to middle infrared luminescence and energy transfer process of Er<sup>3+</sup>/Yb<sup>3+</sup>-co-doped fluorotellurite glasses under different excitations. *Sci. Rep.* **2015**, *5*, 8233. [[CrossRef](#)] [[PubMed](#)]
24. McCumber, D.E. Einstein relations connecting broadband emission and absorption spectra. *Phys. Rev.* **1964**, *136*, A954–A957. [[CrossRef](#)]
25. Várallyay, Z.; Szabó, A.; Rosales, A.; Gonzales, E.; Tobioka, H.; Headley, C. Accurate modeling of cladding pumped, star-shaped, Yb-doped fiber amplifiers. *Opt. Fiber Technol.* **2015**, *21*, 180–186. [[CrossRef](#)]
26. Jeong, Y.; Sahu, J.K.; Payne, D.N.; Nilsson, J. Ytterbium-doped large-core fiber laser with 1.36 kW continuous-wave output power. *Opt. Express* **2004**, *12*, 6088–6092. [[CrossRef](#)] [[PubMed](#)]
27. Supe, A.; Spolitis, S.; Elsts, E.; Murnieks, R.; Doke, G.; Senkans, U.; Matsenko, S.; Grube, J.; Bobrovs, V. Recent developments in cladding-pumped doped fiber amplifiers for telecommunications systems. In Proceedings of the 2020 22nd International Conference on Transparent Optical Networks (ICTON), Bari, Italy, 19–23 July 2020; pp. 1–6.
28. Lee, S.W.; Lee, S.Y.; Pahk, H.J. Precise edge detection method using sigmoid function in blurry and noisy image for TFT-LCD 2D critical dimension measurement. *Curr. Opt. Photonics* **2018**, *2*, 69–78.